Reconstitution of monoterpene indole alkaloid biosynthesis in *Nicotiana benthamiana*

Quentin M. Dudley[1], Seohyun Jo[1], Delia Ayled Serna Guerrero[2], Sarah E. O'Connor[2], Lorenzo Caputi[2]*, Nicola J. Patron[1]*

[1] Engineering Biology, Earlham Institute, Norwich Research Park, Norwich, Norfolk, NR4 7UZ, UK;
[2] Department of Natural Product Biosynthesis, Max Planck Institute for Chemical Ecology, Jena 07745, Germany

*Correspondence: nicola.patron@earlham.ac.uk, lcaputi@ice.mpg.de

Abstract

Monoterpene indole alkaloids (MIAs) are a diverse and important class of plant natural products that include a number of medicinally significant compounds, often present at low concentrations within their native plant species. The complex biosynthesis of MIAs requires the assembly of tryptamine with a secoiridoid to produce the central intermediate, strictosidine, from which all known MIAs derive. Structural complexity makes chemical synthesis challenging, but recent efforts to identify the biosynthetic enzymes provide options for pathway reconstruction in a heterologous host. Previous attempts have had limited success, with yield in microorganisms limited by the poor expression of some enzymes. Here, we reconstitute the pathway for strictosidine biosynthesis from central metabolism without the need for supplementation of any metabolite precursors or intermediates in *Nicotiana benthamiana*. The best yields were obtained by the co-expression of 14 enzymes, of which a major latex protein-like enzyme (MLPL) from *Nepeta* (catmint) was critical for improving flux through the secoiridoid pathway. The production of strictosidine *in planta* expands the range of MIA products amenable to biological synthesis.

Key words: monoterpene indole alkaloid; strictosidine; secologanin; *Catharanthus roseus; Nicotiana benthamiana*

Introduction

Monoterpene indole alkaloids (MIAs) are a large group of plant-produced natural products of which over 3000 have been identified (Pan et al. 2016). This class of molecules includes many medicinally valuable compounds used to treat addiction, heart conditions, dementia, pain, cancer, malaria, and diabetes (**Figure 1**). The best characterised MIA-producing plant is *Catharanthus roseus* (Madagascar periwinkle), which makes over 130 MIAs including the bioactive vinblastine and vincristine used as chemotherapies. However, these valuable molecules are present in low concentrations (0.0005% dry weight) (van Der Heijden et al. 2004), limiting production. Mass cultivation of *C. roseus* cells is feasible, but a high producing cell line has yet to be reported (Saiman et al. 2018). Though methods for transient expression (Yamamoto et al. 2021) and stable genetic transformation (Q. Wang et al. 2012) of *C. roseus* plants have been reported, genetically engineering yield increases within the native plant host remains technically difficult. Furthermore, the structural complexity of many MIAs means chemical synthesis is often challenging (Ishikawa et al. 2009; Kuboyama et al. 2004). Consequently, alternate routes for synthesis are desirable and the recent discovery of missing steps in the vinblastine pathway (Caputi et al. 2018; Qu et al. 2018) makes pathway reconstruction in a heterologous host an increasingly attractive option.

Achieving production of therapeutically useful amounts of MIAs requires pathway engineering to maximise metabolic flux through the early parts of the pathway. Strictosidine is the last common biosynthetic intermediate from which all 3000+ known MIAs derive (**Figure 1**). Reconstitution of its ~11 step biosynthetic pathway in microorganisms can require extensive tuning of enzyme expression conditions and strain optimization (Brown et al. 2015; Billingsley et al. 2017); for example, poor expression of geraniol 8-hydroxylase (G8H) has hampered strictosidine production in yeast (Brown et al. 2015). Achieving useful yields of molecules such as vinblastine, which would require the expression of a further 16+ enzymes beyond strictosidine, is therefore likely to require significant metabolic engineering effort.

The application of synthetic biology approaches to engineering plant systems has facilitated advances in the control and expression of biosynthetic pathways, enabling plants as an alternative production chassis (Patron 2020; Stephenson et al. 2020). A relative of tobacco, *Nicotiana benthamiana* (Bally et al. 2018; Goodin et al. 2008) has emerged as a favoured species for plant-based production of pharmaceutical proteins (Lomonossoff and D'Aoust 2016) and metabolic pathway reconstitution (Stephenson et al. 2020). Successes include gram scale production of triterpenoids (Reed et al. 2017) and milligram scale production of etoposides (Schultz et al. 2019). Indeed, expression in *N. benthamiana* was used by Miettinen and co-workers to reconstitute the *C. roseus* secoiridoid pathway, enabling elucidation of the remaining four missing steps of the pathway (Miettinen et al. 2014). However, they encountered a metabolic bottleneck midway through the 13-step pathway requiring reconstitution in two phases with the latter part requiring provision of an intermediate substrate (iridotrial) in order to obtain strictosidine (Miettinen et al. 2014). In this work, we show that co-expression of additional pathway enzymes enhances nepetalactol production and enables high levels of strictosidine to be produced from the central metabolism *of N. benthamiana* without the need for supplementation of any metabolite precursors or intermediates.

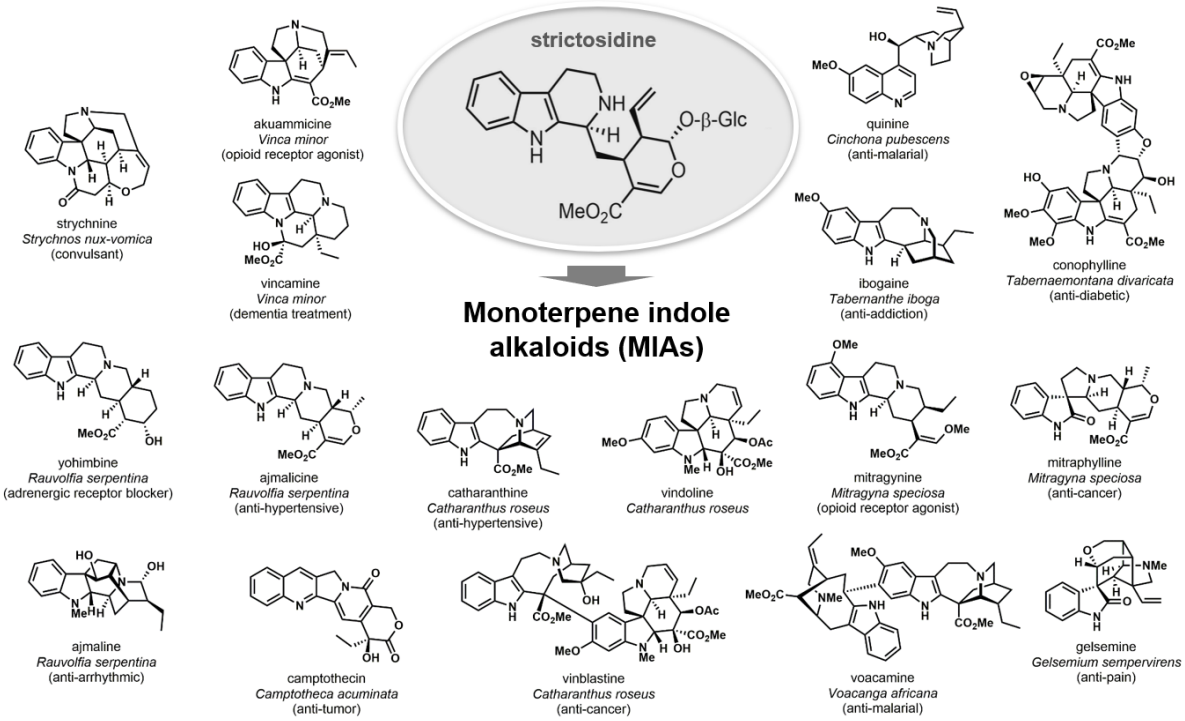

Figure 1. Strictosidine in the last common biosynthetic intermediate for a diverse range of medicinally useful monoterpene indole alkaloids

Methods

DNA Assembly. Binary vectors for *Agrobacterium tumefaciens*-mediated transient expression (agroinfiltration) were assembled using the plant modular cloning toolkit (Engler et al. 2014) and one-step type IIS restriction endonuclease mediated (Golden Gate) assembly protocols as previously described (Cai, Lopez, and Patron 2020). DNA sequences for each pathway enzyme were either synthesised (Twist Bioscience, San Francisco, CA) or amplified from *C. roseus* cDNA by PCR with overhangs containing BpiI (BbsI) recognition sites for assembly into pUAP1 (Addgene #63674). The resulting Level 0 plasmid parts have been domesticated (all endogenous BpiI, BsaI, BsmBI and SapI recognition sites removed) and are flanked by an inverted pair of BsaI recognition sites that produce overhangs compatible with the phytobrick assembly standard (Patron et al. 2015) (**Supplementary Table S1**). To create plasmids for transient expression in *N. benthamiana,* Level 0 parts encoding the coding sequence were assembled into Level 1 acceptors in a one-step cloning reaction (Cai, Lopez, and Patron 2020) with Level 0 parts encoding regulatory elements to enable constitutive expression and, when required, a synthetic chloroplast transit peptide sequence (**Supplementary Table S2**). All plasmids, as well with plasmid maps of their entire sequence, have been submitted to the Addgene repository.

Transient expression in *N. benthamiana*. *N. benthamiana* plants were grown in a controlled environment room with 16 hr light, 8 hr hours dark with room at 22 °C, 80% humidity, and ~200 µmol/m^2/s light intensity. *A. tumefaciens* GV3101 was transformed with the binary plasmid encoding the gene of interest and an individual colony used to inoculate liquid LB medium containing 50 µg/mL rifampicin, 20 µg/mL gentamicin plus the appropriate antibiotic for maintenance of the binary plasmid (100 µg/mL carbenicillin, 50 µg/mL kanamycin, or 100 µg/mL spectinomycin). Overnight saturated cultures were centrifuged at 3,400 *x g* for 30 min at room temperature and cells were resuspended in infiltration medium (10 mM 2-(N-morpholino)ethanesulfonic acid (MES) pH 5.7, 10 mM $MgCl_2$, 200 µM 3′,5′-Dimethoxy-4′-hydroxyacetophenone (acetosynringone)) and incubated at room temperature for 2-3 hours with slow shaking. All resuspended cultures were diluted to 0.8 OD_{600nm} and mixed in equal ratios as dictated by the experimental condition. An *A. tumefaciens* strain encoding a gene expressing the P19 suppressor of gene silencing from Tomato Bushy Stunt Virus (TBSV) previously shown to increase heterologous expression was included in every infiltration (Sainsbury, Thuenemann, and Lomonossoff 2009). Healthy plants (29-37 days old) with 3-4 fully expanded true leaves were infiltrated on the abaxial side of the leaf using a 1 mL needleless syringe and grown for five days in a MLR-352-PE plant growth chamber (Panasonic Healthcare Co, Oizumi-Machi, Japan) with 16 hr light, 8 hr hours dark at 22 °C and 120-180 µmol/m^2/s light intensity. All chemical compounds were purchased from Sigma-Aldrich (St. Louis, MO).

Metabolite extraction. Five days post-infiltration, 100-300 mg of infiltrated *N. benthamiana* leaf tissue was collected in 1.5 mL microcentrifuge tubes and flash frozen on liquid nitrogen. Leaf tissue was lyophilised overnight using a VirTis BenchTop SLC freeze dryer (SP Industries, Stone Ridge NY, USA) set to -49 °C and 300 mTorr. Samples were then ground to powder using a 3 mm tungsten carbide bead (Qiagen Cat. No. / ID: 69997) on a TissueLyser II (Qiagen, Hilden, Germany) set to 20 Hz for 20 sec. Lyophilised leaf tissue was extracted with 70% methanol + 0.1% formic acid (1:100, w:v). The solvent contained 10 µM of harpagoside (Extrasyntheses) as internal standard. The extractions were performed at room temperature for 1 hr, with 10 min sonication and 50 min constant shaking. Samples were centrifuged at 17,000 *x g* for 10 min to separate the debris and filtered through 0.2 µm PTFE disk filters before UPLC/MS analysis.

Metabolite analysis. UPLC/MS analysis was performed on an Impact II qTOF mass spectrometer (Bruker) coupled to an Elute UPLC (Bruker) chromatographic system. Chromatographic separation was carried out on a Phenomenex Kinetex column XB-C18 (100 × 2.10 mm, 2.6 µm particle size) kept at 40 °C and the binary solvent system consisted of solvent A (H_2O + 0.1% formic acid) and solvent B (acetonitrile). Flow rate was 600 µL/min. The column was equilibrated with 99% A and 1% B. During the first minute of chromatography, solvent B reached 5%. Then a linear gradient from 5% B to 40% B in 5 min allowed the separation of the compounds of interest. The column was then washed at 100% B for 1.5 min and re-equilibrated to 1% B. Injection volume was 2 µL.

Mass spectrometry was performed both in positive and negative ion mode with a scan range *m/z* 100–1000. The mass spectrometer was calibrated using sodium formate adducts. The source settings were the following: capillary voltage 3.5 kV, nebulizer 2.5 Bar, dry gas 11.0 L/min, dry temperature 250 °C. Data analysis was performed using the Bruker Data Analysis software.

Quantification of 7-deoxyloganic acid (7-DLA), loganin, loganic acid and strictosidine was based on calibration curves generated using pure compounds. Loganin and loganic acid were purchased from Sigma. 7-deoxyloganic acid was synthesised according to the method previously described (Rodríguez-López et al. 2021). Strictosidine was synthesised and purified as previously described (Stavrinides et al. 2016). The standards were diluted in 70% methanol + 0.1% formic acid to give nine calibrants with concentrations between 40 nM and 10 µM. A linear response was observed for all compounds in this range of concentrations (R^2>0.993).

Results

MLPL1 from *Nepeta mussinii* is essential for 7-DLA production in *N. benthamiana.*

We transiently expressed pathway enzymes by co-infiltrating *N. benthamiana* with a mixture of *A. tumefaciens* strains with each containing a plasmid encoding a single step of the pathway to produce 7-DLA (**Figure 2**). To enhance the pool of geraniol pyrophosphate (GPP) substrate from the plastidial 2-C-methyl-D-erythritol 4-phosphate/1-deoxy-D-xylulose 5-phosphate (MEP/DOXP) pathway, we included a bifunctional geranyl/geranylgernayl pyrophosphate synthase (GPPS/GGPPS from *Picea abies* (Schmidt et al. 2010) also utilised by (Miettinen et al. 2014). In previous experiments, co-expression of 1-deoxy-D-xylulose 5-phosphate synthase (DXS) was shown to aid production of the diterpenoids cembratrien-ol (Brückner and Tissier 2013) and taxadiene (Li et al. 2019). Therefore, to further enhance the pool of isoprenoid substrates, we also expressed DXS from *C. roseus*. We added a previously characterised synthetic plastid transit peptide (Engler et al. 2014) to the N-terminus of DXS, GPPS and geraniol synthase (GES). We found that the transient expression of DXS, GPPS and GES produces a range of non-volatile glycosylated and oxidised derivates of geraniol (**Supplementary Figure S1**), consistent with previous studies (Miettinen et al. 2014; Dong et al. 2016).

The biosynthetic pathway for production of *cis-trans* nepetalactone in the genus *Nepeta* overlaps the secoiridoid pathway from *C. roseus* up to the stereoselective reduction of 8-oxogeranial to an enol intermediate by the NADPH-dependent iridoid synthase (ISY) (Geu-Flores et al. 2012). It has recently been shown that ISY works in combination with nepetalactol-related short-chain dehydrogenase-reductases (NEPS) and a major latex protein-like enzyme (MLPL) to control of stereospecificity of the ring closure (Lichman et al. 2019; 2020). We therefore hypothesised that addition of the MLPL from *Nepeta mussinii* (a.k.a *Nepeta racemosa*), which is specific for the stereochemistry found in strictosidine, would enhance flux through the secoiridoid pathway reconstituted in *N. benthamiana*

Expression of DXS, GPPS, GES, G8H, 8-hydroxygeraniol oxidoreductase (GOR), ISY, and MLPL further modified the profile of derivatised pathway intermediates (**Supplementary Figure S1**). Infiltration of the full 7-DLA pathway without MLPL does not produce a peak for 7-DLA (359 *m/z*) or acylated 7-DLA (401 *m/z*) as found in (Miettinen et al. 2014) (**Figure 2**). However, the inclusion of MLPL produces a clear peak of 359 *m/z* which matches the retention time of the 7-DLA standard. Exclusion of 7-deoxyloganetic acid glucosyl transferase (7-DLGT) produces a peak of 359 *m/z* but this does not match the retention time of 7-DLA. It is possible that endogenous glycosyltransferases (GTs) from *N. benthamiana* are able to use 7-deoxyloganetic acid to produce a glucose ester; importantly, the high expression of 7-DLGT compared to endogenous GTs mean that this putative glucose ester peak is not present in the spectra of the full 7-DLA pathway.

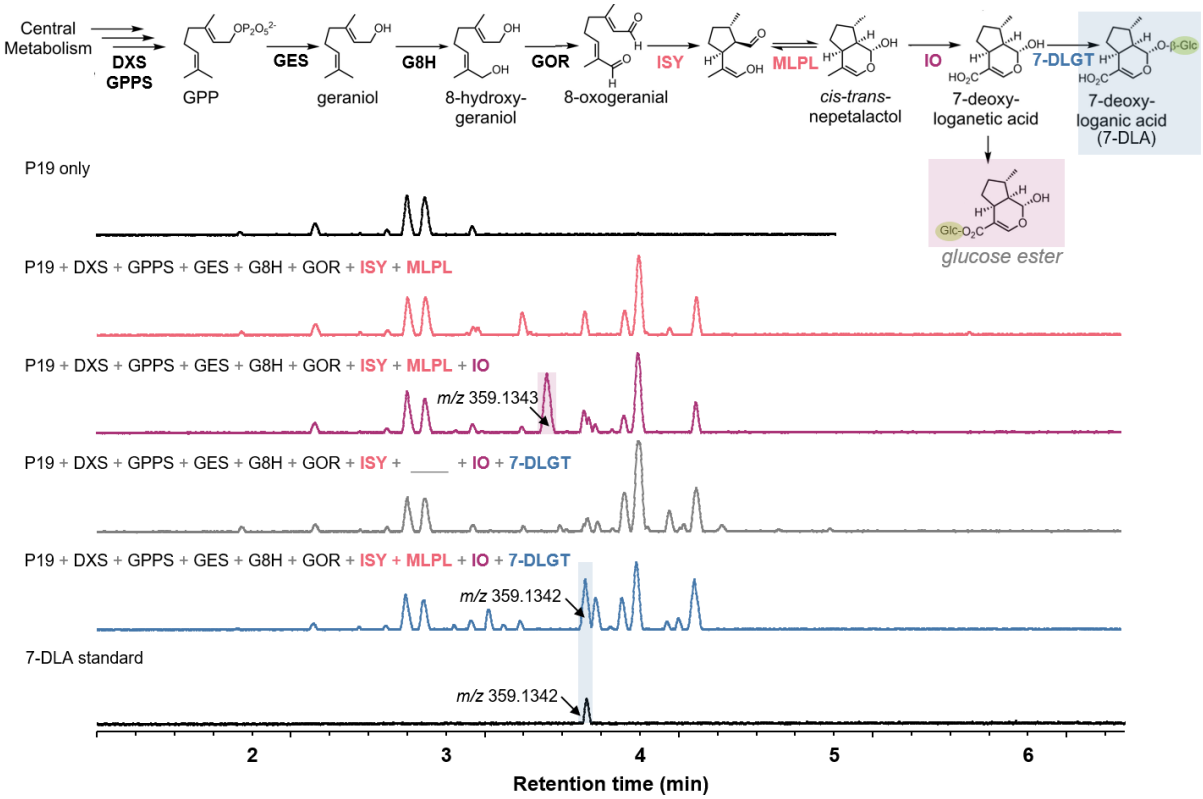

Figure 2. MLPL1 from *Nepeta mussinii* enables 7-deoxyloganic acid production in *N. benthamiana*. Individual strains of *A. tumefaciens*, each containing a plasmid encoding a single pathway enzyme, were mixed in equal ratios and co-infiltrated into *N. benthamiana* leaves. Transient expression of all pathway enzymes plus MLPL produces a peak of 359.13 *m/z* which matches the mass and retention time of a 7-deoxyloganic acid (7-DLA) standard. The reconstituted pathway without DLGT also produces a 359.13 *m/z* peak but at a different retention time, likely due to endogenous glycosyltransferases *of N. benthamiana* producing the glucose ester of 7-deoxyloganetic acid. DXS, 1-deoxy-D-xylulose 5-phosphate synthase; GPPS, geranyl diphosphate synthase; GES, geraniol synthase; G8H, geraniol 8-oxidase; GOR, 8-hydroxygeraniol oxidoreductase; ISY, iridoid synthase; MLPL, major latex protein–like; IO, iridoid oxidase; 7-DLGT, 7-deoxyloganetic acid glucosyl transferase

Reconstitution of the complete strictosidine pathway.

Building on the experimental conditions which produced 7-DLA, we sequentially added the remaining five pathway enzymes and measured the pathway intermediates at each stage (**Figure 3A, Supplementary Figure S2-S6**). Co-infiltration of strains expressing enzymes for the entire pathway produces a distinct peak at 531 *m/z* matching the strictosidine standard (**Figure 3C, Supplementary Figure S5**); this pathway configuration produces 4.29 ± 2.00 µM of strictosidine which correlates to 0.23 ± 0.11 mg strictosidine / g dry weight leaf tissue (0.023% DW). The accumulation of loganin suggests secologanin synthase is a bottleneck step. This is in contrast to previous data suggesting that loganic acid O-methyltransferase (LAMT), which has a low substrate affinity (K_m = 12.5–14.8 mM) (Madyastha et al. 1973; Murata et al. 2008), might be a rate-limiting step of the late stages of the secoiridoid pathway. In addition to the substantial peak corresponding to strictosidine, transient expression of the full pathway also produces a smaller peak (**Figure 3C, Supplementary Figure S6**) with a mass shift of 86 Da from strictosidine, suggesting that this may be a malonylated derivative of strictosidine produced by endogenous *N. benthamiana* acyltransferases.

Transient expression of the strictosidine pathway without DXS, GPPS, and MLPL (**Figure 3B**) confirms the beneficial effect of these enzymes. Addition of MLPL increases strictosidine production >60 fold while supplementation of GPPS improves yield ~5 fold. DXS supplementation did not change the amount of strictosidine produced, however, it does produce additional derivatives of geraniol (**Supplementary Figure S1**).

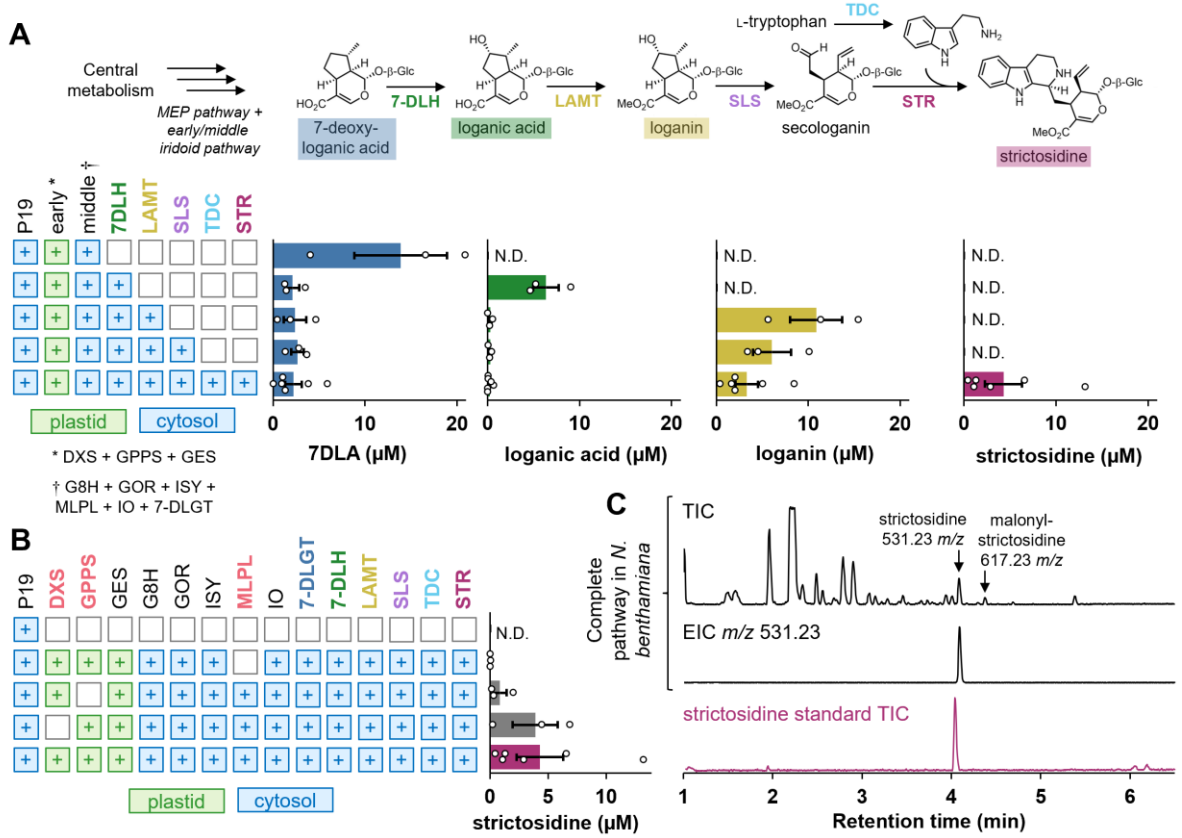

Figure 3. Complete reconstitution of strictosidine biosynthesis in *N. benthamiana*. (A) Quantification of intermediates and final product strictosidine by UPLC/MS analysis. (B) Absence of MLPL reduces strictosidine production >60 fold while supplementation of GPPS improves yield ~5 fold. (C) the total ion chromatogram of leaf tissue infiltrated with entire pathway to strictosidine (including DXS, GPPS, and MLPL). The peak at 4.09 min retention time in the TIC and extracted ion chromatogram at 531.23 *m/z* matches a strictosidine standard. N.D., not detected; 7-DLH, 7-deoxyloganic acid hydroxylase; LAMT, loganic acid O-methyltransferase; SLS, secologanin synthase; TDC, tryptophan decarboxylase; STR, strictosidine synthase. Values and error bars represent the mean and the standard error of n=3 or n=6 biological independent leaf samples.

Mimicking *C. roseus* subcellular compartmentalisation maximises strictosidine production.

To compare the effect of chloroplast and cytosolic enzyme localisation on yields of 7-DLA and strictosidine production, we added (or removed in the case of GPPS/GES) a transit peptide to each enzyme (**Figure 4**). To enhance flux of isoprenoid precursors in the cytosol, we aimed to alleviate the rate limiting step of the mevalonate pathway by co-infiltrating a truncated 3-hydroxy-3-methylglutaryl-coenzyme A reductase (tHMGR) from oat, previously shown to improve titres of the triterpenoid β-amyrin in *N. benthamiana* (Reed et al. 2017). When all enzymes are localised to the cytosol, flux through the secoiridoid pathway is minimal (~90-fold reduction for 7-DLA) while localisation of all pathway enzymes to the chloroplast results in 5-fold less 7-DLA (**Figure 4A**). The best yields of 7-DLA (**Figure 4A**) and strictosidine (**Figure 4B**) were obtained with chloroplast localisation of the early pathway and cytosolic localisation of subsequent steps. Production of 7-DLA in the chloroplast is possibly limited by the availability of partner P450 reductases for G8H and iridoid oxidase (IO) or small molecule substrates such as UDP-glucose for 7-DLGT, however, all possible divisions of pathway enzymes between the cytosol and chloroplast still produce 7-DLA indicating that pathway intermediates can cross the chloroplast membrane.

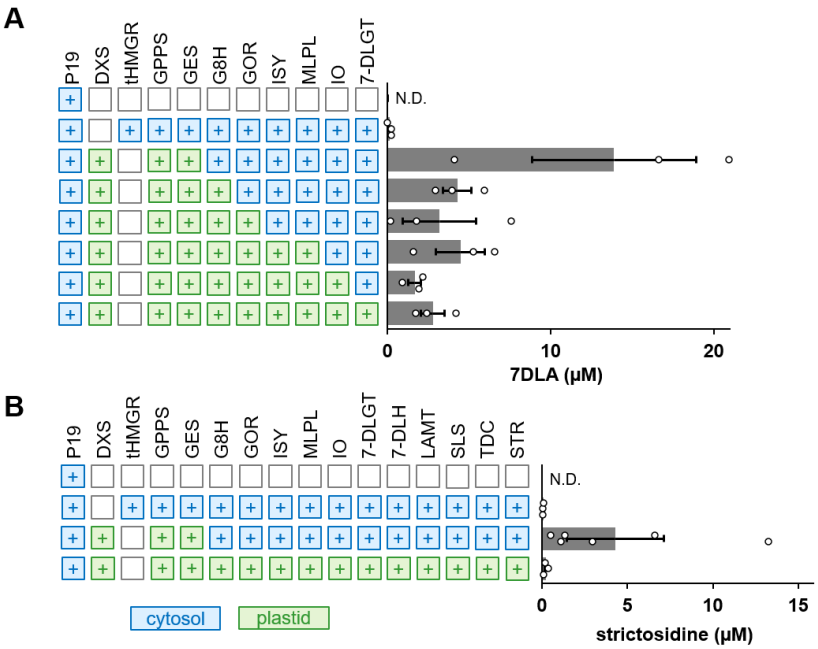

Figure 4. Relocation of 7-DLA (A) and strictosidine (B) biosynthesis genes to the cytosol (blue) or the chloroplast (green) decreases product yield. tHMGR, truncated 3-hydroxy-3-methylglutaryl-coenzyme A reductase. Values and error bars represent the mean and the standard error of n=3 or n=6 biological independent leaf samples.

Discussion

In this work, we provide the first report of high quantities of strictosidine (0.23 ± 0.11 mg/g DW) produced from central metabolism in a photosynthetic organism. Plants from the mint family (Lamiaceae) produce a range of iridoid products (Boachon et al. 2018); the genus *Nepeta* L., colloquially known as catnip or catmint, use the early part of the secoiridoid pathway to produce nepetalactones for insect defence which are also responsible for the euphoric effects on cats. Recent work revealed that NEPS controls the stereospecificity of the ring closure (Lichman et al. 2019) and that production of *cis-trans* nepetalactol is assisted by MLPL (Lichman et al. 2020). The heterologous expression of MLPL from *N. mussinii* to assist with cyclisation of the reactive enol product of ISY overcame bottlenecks in the secoiridoid pathway (**Figure 2**) and was critical for enabling heterologous production of strictosidine in *N. benthamiana* (**Figure 3**). We hypothesise that MLPL might similarly enhance secoiridoid metabolic engineering in microorganisms such as yeast (Brown et al. 2015). Indeed, a cell-free *in vitro* one-pot enzyme cascade included MLPL with nine other pathway enzymes, accessory proteins, and cofactor regeneration enzymes to produce ~1 g/L nepetalactone (Bat-Erdene et al. 2021).

The MIA pathway in *C. roseus* is highly compartmentalised across both sub-cellular compartments and cell types. The first committed step is geraniol synthesis (GES), which is localised to the chloroplast of internal phloem-associated parenchyma (IPAP) cells (Simkin et al. 2013). To increase substrate availability for GES, we co-expressed GPPS from *P. abies* and DXS from *C. roseus*. Expression of chloroplast-targeted PaGPPS improved yield ~5 fold (**Figure 3**) in similarity with previously reported effects on the production of geraniol (Dong et al. 2016). Of note, PaGPPS is nearly identical (**Supplementary Figure S7**) to a GPPS from *Picea glauca* shown *in vitro* to produce higher levels of the monoterpene limonene relative to six other GPPS sequences commonly used in terpene metabolic engineering (Dudley et al. 2020). Interestingly, DXS had relatively little effect on the yield of strictosidine in contrast to previously reported effects on the production of diterpenoids (Brückner and Tissier 2013; Li et al. 2019).

Recent efforts to engineer metabolic pathways have found benefits in altering the compartmentalisation of pathway enzymes (Jensen and Scharff 2019; Dong et al. 2016). For example, the pathway to produce the cyanogenic glucoside dhurrin was relocated to the chloroplast of *Nicotiana tabacum* where ferredoxin, reduced via the photosynthetic electron transport chain, can

serves as an efficient electron donor to the two cytochromeP450s (CYPs) within the pathway (Gnanasekaran et al. 2016). Additionally, the localisation of enzymes encoding the late steps of the artemisinin pathway to the chloroplast in *N. tabacum* produced higher levels of artemisinin (800 µg/g DW) (Malhotra et al. 2016) and artemisinic acid (~1200 µg/g DW) (Fuentes et al. 2016) compared to localisation within the cytosol (6.8 µg/g DW artemisinin) (Farhi et al. 2011). This increase is possibly due to the isolation of metabolites from the cytosol where they may both impact viability and be exposed to unwanted derivatisation by endogenous glycosyltransferases (van Herpen et al. 2010; Ting et al. 2013; B. Wang et al. 2016). Production of halogenated indican (Fräbel et al. 2018) and vanillin (Gallage et al. 2018) in *N. benthmaiana* also benefited from chloroplast localisation. In contrast, a recent report found that production of diterpenoids (typically synthesised in the chloroplast) was dramatically enhanced by co-opting the cytosolic mevalonate pathway to produce GGPP rather than the chloroplast MEP pathway (De La Peña and Sattely 2021).

In this study, we found that the optimal configuration for reconstruing the pathway to strictosidine within *N. benthamiana* leaves is to match the *C. roseus* strategy of utilising the chloroplast MEP pathway for isoprenoid precursors to produce geraniol and then localising the remaining pathway enzymes in the cytosol (**Figure 4**). We hypothesise that monoterpene production in the cytosol is limited since GPP (10 carbons) produced by GPPS is also the substrate for the *N. benthamiana* farnesylpyrophosphate synthase (FPPS), which produces farnesylpyrophosphate (FPP) (15 carbons). Supporting this hypothesis is data suggesting that all four copies of NbFPPS are upregulated to produce sesquiterpenoid phytosterols and phytoalexins in response to *Phytophthora infestans* (Rin et al. 2020). *A. tumefaciens* also elicits widespread transcriptional remodelling when infiltrated into *N. benthamiana* (Grosse-Holz et al. 2018). This competition between GES and FPPS might also explain the higher levels of geraniol and geraniol derivatives in the plastid reported by (Dong et al. 2016). Future efforts to conditionally inactivate NbFPPS during heterologous production might enable a metabolic engineering strategy that could take advantage of both the plastid and cytosolic route to geraniol production.

In *C. roseus*, geraniol diffuses (or is transported) from the plastid into the cytosol to react with G8H bound to the exterior of the ER membrane. The next steps (G8H to deoxyloganic acid hydroxylase (7-DLH)) are active in the cytosol of IPAP cells with two CYPs (G8H and IO) anchored to the ER membrane (Miettinen et al. 2014). Loganic acid is then transported by NPF2.4/5/6 (Larsen et al. 2017) to epidermal cells where four more enzymes (LAMT to strictosidine synthase (STR)) produce strictosidine (Yamamoto et al. 2016; 2019). Strictosidine accumulates in the vacuole with export mediated by NPF2.9 (Payne et al. 2017). Thus, four pathway CYPs (G8H, IO, 7-DLH and secologanin synthase (SLS)) are likely interfacing with endogenous *N. benthamiana* CYP reductases for electron transfer of NADPH to the CYPs. It is possible that the necessary CYP reductases are less abundant in the chloroplast and thus limit the accumulation of strictosidine in this compartment. It is also possible that the CYP450s are improperly membrane anchored or that higher stromal pH of the chloroplast (~8.0)(Song et al. 2004) inhibits enzyme activity compared to the cytosol (pH ~7.0). We also considered if lack of an additional cofactor for LAMT, S-Adenosyl methionine (SAM) explains the low levels of strictosidine production (relative to 7-DLA) in the chloroplast. However, this small molecule is known to be actively transported into the plastid (Linka and Weber 2010) and is an essential substrate for ChlM (Mg-protoporphyrin IX methyltransferase) involved in chlorophyll biosynthesis within the chloroplast.

The production of strictosidine *in planta* opens up a wealth of MIA products to biological synthesis. Particularly as new biosynthesis pathways for additional MIAs are discovered (e.g. the anti-addictive compound ibogaine (Farrow et al. 2019), the antimalarial quinine (Trenti et al. 2021)), the possibility of coupling this work in a plug-and-play manner with downstream biosynthesis modules is an exciting prospect for natural product synthesis.

Supplementary data

Supplementary Figure S1. Early metabolites of the iridoid pathway are derivatised by endogenous enzymes from *N. benthamiana*.
Supplementary Figure S2. Detection of 7-deoxyloganic acid by transient expression in *N. benthamiana*
Supplementary Figure S3. Detection of loganic acid by transient expression in *N. benthamiana*
Supplementary Figure S4. Detection of loganin by transient expression in *N. benthamiana*
Supplementary Figure S5. Detection of strictosidine by transient expression in *N. benthamiana*

Supplementary Figure S6. Detection of malonyl-strictosidine by transient expression in *N. benthamiana*
Supplementary Figure S7. Amino acid sequence alignment of candidate GPPS enzymes
Supplemental Table S1. Enzymes and L0 plasmid parts built in this study
Supplemental Table S2. Level 1 plasmids for *A. tumefaciens* - mediated transient expression in N. benthamiana

Author Contributions

Q.M.D., S.E.O., L.C, and N.J.P. conceived the study. Q.M.D performed DNA assembly and transient expression with assistance from S.J., D.A.S.G and L.C. performed metabolite extraction and analysis. Q.M.D., S.E.O., N.J.P., and L.C. wrote the manuscript. S.E.O. and N.J.P obtained funding and provided supervision.

ORCID

Quentin M. Dudley (0000-0002-2987-5172)
Seohyun Jo (0000-0001-5742-2376)
Sarah E. O'Connor (0000-0003-0356-6213)
Lorenzo Caputi (0000-0002-7783-6733)
Nicola J. Patron (0000-0002-8389-1851)

Acknowledgements

We thank Nat Sherden for help with plasmid construction and Benjamin Lichman for guidance working with MLPL. pL0-AstHMGR was a generous gift from Anne Osbourn.

Data Availability

Plasmids will be available from Addgene (submission in progress).

Funding

The authors gratefully acknowledge the support of the Biotechnology and Biological Sciences Research Council (BBSRC). This research was funded by the BBSRC Strategic Programme Grant 'Genomes to Food Security' (BB/CSP1720/1) and an industrial partnership award with Leaf Expression Systems (BB/P010490/1). The funders had no role in study design, data collection and analysis, decision to publish, or preparation of the manuscript.

Conflict of interest statement

None declared

References

Bally, Julia, Hyungtaek Jung, Cara Mortimer, Fatima Naim, Joshua G. Philips, Roger Hellens, Aureliano Bombarely, Michael M. Goodin, and Peter M. Waterhouse. 2018. "The Rise and Rise of Nicotiana Benthamiana: A Plant for All Reasons." *Annual Review of Phytopathology* 56: 405–26. https://doi.org/10.1146/annurev-phyto-080417-050141.

Bat-Erdene, Undramaa, John M Billingsley, William C Turner, Benjamin R Lichman, Francesca M Ippoliti, Neil K Garg, Sarah E O'Connor, and Yi Tang. 2021. "Cell-Free Total Biosynthesis of Plant Terpene Natural Products Using an Orthogonal Cofactor Regeneration System." *ACS Catalysis* 11: 9898–9903. https://doi.org/10.1021/acscatal.1c02267.

Billingsley, John M., Anthony B. DeNicola, Joyann S. Barber, Man Cheng Tang, Joe Horecka, Angela Chu, Neil K. Garg, and Yi Tang. 2017. "Engineering the Biocatalytic Selectivity of Iridoid Production in Saccharomyces Cerevisiae." *Metabolic Engineering* 44 (August): 117–25. https://doi.org/10.1016/j.ymben.2017.09.006.

Boachon, Benoît, C. Robin Buell, Emily Crisovan, Natalia Dudareva, Nicolas Garcia, Grant Godden, Laura Henry, et al. 2018. "Phylogenomic Mining of the Mints Reveals Multiple Mechanisms Contributing to the Evolution of Chemical Diversity in Lamiaceae." *Molecular Plant* 11 (8): 1084–96. https://doi.org/10.1016/j.molp.2018.06.002.

Brown, Stephanie, Marc Clastre, Vincent Courdavault, and Sarah E. O'Connor. 2015. "De Novo Production of the Plant-Derived Alkaloid Strictosidine in Yeast." *Proceedings of the National Academy of Sciences of the United States of America* 112 (11): 3205–10. https://doi.org/10.1073/pnas.1423555112.

Brückner, Kathleen, and Alain Tissier. 2013. "High-Level Diterpene Production by Transient

Expression in Nicotiana Benthamiana." *Plant Methods* 9 (46).
Cai, Yao-Min, Jose A. Carrasco Lopez, and Nicola J. Patron. 2020. "Phytobricks: Manual and Automated Assembly of Constructs for Engineering Plants." In *DNA Cloning and Assembly*, edited by Sunila Chandaran and Kevin W. George, 179–99. New York, NY: Humana. http://link.springer.com/10.1007/978-1-62703-764-8.
Caputi, Lorenzo, Jakob Franke, Scott C. Farrow, Khoa Chung, Richard M.E. Payne, Trinh Don Nguyen, Thu Thuy T. Dang, et al. 2018. "Missing Enzymes in the Biosynthesis of the Anticancer Drug Vinblastine in Madagascar Periwinkle." *Science* 360 (6394): 1235–39. https://doi.org/10.1126/science.aat4100.
Dong, Lemeng, Esmer Jongedijk, Harro Bouwmeester, and Alexander Van Der Krol. 2016. "Monoterpene Biosynthesis Potential of Plant Subcellular Compartments." *New Phytologist* 209 (2): 679–90. https://doi.org/10.1111/nph.13629.
Dudley, Quentin M., Ashty S. Karim, Connor J. Nash, and Michael C. Jewett. 2020. "In Vitro Prototyping of Limonene Biosynthesis Using Cell-Free Protein Synthesis." *Metabolic Engineering* 61 (May): 251–60. https://doi.org/10.1016/j.ymben.2020.05.006.
Engler, Carola, Mark Youles, Ramona Gruetzner, Tim Martin Ehnert, Stefan Werner, Jonathan D.G. Jones, Nicola J. Patron, and Sylvestre Marillonnet. 2014. "A Golden Gate Modular Cloning Toolbox for Plants." *ACS Synthetic Biology* 3 (11): 839–43. https://doi.org/10.1021/sb4001504.
Farhi, Moran, Elena Marhevka, Julius Ben-Ari, Anna Algamas-Dimantov, Zhuobin Liang, Vardit Zeevi, Orit Edelbaum, et al. 2011. "Generation of the Potent Anti-Malarial Drug Artemisinin in Tobacco." *Nature Biotechnology* 29 (12): 1072–74. https://doi.org/10.1038/nbt.2054.
Farrow, Scott C., Mohamed O. Kamileen, Lorenzo Caputi, Kate Bussey, Julia E.A. Mundy, Rory C. McAtee, Corey R.J. Stephenson, and Sarah E. O'Connor. 2019. "Biosynthesis of an Anti-Addiction Agent from the Iboga Plant." *Journal of the American Chemical Society* 141 (33): 12979–83. https://doi.org/10.1021/jacs.9b05999.
Fräbel, Sabine, Bastian Wagner, Markus Krischke, Volker Schmidts, Christina M. Thiele, Agata Staniek, and Heribert Warzecha. 2018. "Engineering of New-to-Nature Halogenated Indigo Precursors in Plants." *Metabolic Engineering* 46 (December 2017): 20–27. https://doi.org/10.1016/j.ymben.2018.02.003.
Fuentes, Paulina, Fei Zhou, Alexander Erban, Daniel Karcher, Joachim Kopka, and Ralph Bock. 2016. "A New Synthetic Biology Approach Allows Transfer of an Entire Metabolic Pathway from a Medicinal Plant to a Biomass Crop." *ELife* 5: e13664. https://doi.org/10.7554/eLife.13664.
Gallage, Nethaji J., Kirsten Jørgensen, Christian Janfelt, Agnieszka J.Z. Nielsen, Thomas Naake, Eryk Duński, Lene Dalsten, Michel Grisoni, and Birger Lindberg Møller. 2018. "The Intracellular Localization of the Vanillin Biosynthetic Machinery in Pods of Vanilla Planifolia." *Plant and Cell Physiology* 59 (2): 304–18. https://doi.org/10.1093/pcp/pcx185.
Geu-Flores, Fernando, Nathaniel H. Sherden, Vincent Courdavault, Vincent Burlat, Weslee S. Glenn, Cen Wu, Ezekiel Nims, Yuehua Cui, and Sarah E. O'Connor. 2012. "An Alternative Route to Cyclic Terpenes by Reductive Cyclization in Iridoid Biosynthesis." *Nature* 492 (7427): 138–42. https://doi.org/10.1038/nature11692.
Gnanasekaran, Thiyagarajan, Daniel Karcher, Agnieszka Zygadlo Nielsen, Helle Juel Martens, Stephanie Ruf, Xenia Kroop, Carl Erik Olsen, et al. 2016. "Transfer of the Cytochrome P450-Dependent Dhurrin Pathway from Sorghum Bicolor into Nicotiana Tabacum Chloroplasts for Light-Driven Synthesis." *Journal of Experimental Botany* 67 (8): 2495–2506. https://doi.org/10.1093/jxb/erw067.
Goodin, Michael M., David Zaitlin, Rayapati A. Naidu, and Steven A. Lommel. 2008. "Nicotiana Benthamiana: Its History and Future as a Model for Plant-Pathogen Interactions." *Molecular Plant-Microbe Interactions* 21 (8): 1015–26. https://doi.org/10.1094/MPMI-21-8-1015.
Grosse-Holz, Friederike, Steven Kelly, Svenja Blaskowski, Farnusch Kaschani, Markus Kaiser, and Renier A.L. van der Hoorn. 2018. "The Transcriptome, Extracellular Proteome and Active Secretome of Agroinfiltrated Nicotiana Benthamiana Uncover a Large, Diverse Protease Repertoire." *Plant Biotechnology Journal* 16 (5): 1068–84. https://doi.org/10.1111/pbi.12852.
Heijden, Robert van Der, Denise I Jacobs, Wim Snoeijer, Didier Hallard, and Robert Verpoorte. 2004. "The Catharanthus Alkaloids: Pharmacognosy and Biotechnology." *Current Medicinal Chemistry* 11 (5): 607–28. https://doi.org/10.2174/0929867043455846.
Herpen, Teun W.J.M. van, Katarina Cankar, Marilise Nogueira, Dirk Bosch, Harro J. Bouwmeester, and Jules Beekwilder. 2010. "Nicotiana Benthamiana as a Production Platform for Artemisinin Precursors." *PLoS ONE* 5 (12). https://doi.org/10.1371/journal.pone.0014222.
Ishikawa, Hayato, David A. Colby, Shigeki Seto, Porino Va, Annie Tam, Hiroyuki Kakei, Thomas J. Rayl, Inkyu Hwang, and Dale L. Boger. 2009. "Total Synthesis of Vinblastine, Vincristine,

Related Natural Products, and Key Structural Analogues." *Journal of the American Chemical Society* 131 (13): 4904–16. https://doi.org/10.1021/ja809842b.

Jensen, Poul Erik, and Lars B. Scharff. 2019. "Engineering of Plastids to Optimize the Production of High-Value Metabolites and Proteins." *Current Opinion in Biotechnology* 59: 8–15. https://doi.org/10.1016/j.copbio.2019.01.009.

Kuboyama, Takeshi, Satoshi Yokoshima, Hidetoshi Tokuyama, and Tohru Fukuyama. 2004. "Stereocontrolled Total Synthesis of (+)-Vincristine." *Proceedings of the National Academy of Sciences* 101 (33): 11966–70. https://doi.org/10.1016/j.tetasy.2008.12.020.

La Peña, Ricardo De, and Elizabeth S. Sattely. 2021. "Rerouting Plant Terpene Biosynthesis Enables Momilactone Pathway Elucidation." *Nature Chemical Biology* 17 (2): 205–12. https://doi.org/10.1038/s41589-020-00669-3.

Larsen, Bo, Victoria L. Fuller, Jacob Pollier, Alex Van Moerkercke, Fabian Schweizer, Richard Payne, Maite Colinas, Sarah E. O'Connor, Alain Goossens, and Barbara A. Halkier. 2017. "Identification of Iridoid Glucoside Transporters in Catharanthus Roseus." *Plant and Cell Physiology* 58 (9): 1507–18. https://doi.org/10.1093/pcp/pcx097.

Li, Jianhua, Ishmael Mutanda, Kaibo Wang, Lei Yang, Jiawei Wang, and Yong Wang. 2019. "Chloroplastic Metabolic Engineering Coupled with Isoprenoid Pool Enhancement for Committed Taxanes Biosynthesis in Nicotiana Benthamiana." *Nature Communications* 10 (1): 1–12. https://doi.org/10.1038/s41467-019-12879-y.

Lichman, Benjamin R., Grant T. Godden, John P. Hamilton, Lira Palmer, Mohamed O. Kamileen, Dongyan Zhao, Brieanne Vaillancourt, et al. 2020. "The Evolutionary Origins of the Cat Attractant Nepetalactone in Catnip." *Science Advances* 6 (20). https://doi.org/10.1126/sciadv.aba0721.

Lichman, Benjamin R., Mohamed O. Kamileen, Gabriel R. Titchiner, Gerhard Saalbach, Clare E.M. Stevenson, David M. Lawson, and Sarah E. O'Connor. 2019. "Uncoupled Activation and Cyclization in Catmint Reductive Terpenoid Biosynthesis." *Nature Chemical Biology* 15 (1): 71–79. https://doi.org/10.1038/s41589-018-0185-2.

Linka, Nicole, and Andreas P.M. Weber. 2010. "Intracellular Metabolite Transporters in Plants." *Molecular Plant* 3 (1): 21–53. https://doi.org/10.1093/mp/ssp108.

Lomonossoff, George P., and Marc André D'Aoust. 2016. "Plant-Produced Biopharmaceuticals: A Case of Technical Developments Driving Clinical Deployment." *Science* 353 (6305): 1237–40. https://doi.org/10.1126/science.aaf6638.

Madyastha, K. Madhava., Rocco. Guarnaccia, Claire. Baxter, and Carmine. J. Coscia. 1973. "S-Adenosyl-L-Methionine: Loganic Acid Methyltransferase. A Carboxyl-Alkylating Enzyme from Vinca Rosea." *Journal of Biological Chemistry* 248 (7): 2497–2501. https://doi.org/10.1016/S0021-9258(19)44136-7.

Malhotra, Karan, Mayavan Subramaniyan, Khushboo Rawat, Md Kalamuddin, M. Irfan Qureshi, Pawan Malhotra, Asif Mohmmed, Katrina Cornish, Henry Daniell, and Shashi Kumar. 2016. "Compartmentalized Metabolic Engineering for Artemisinin Biosynthesis and Effective Malaria Treatment by Oral Delivery of Plant Cells." *Molecular Plant* 9 (11): 1464–77. https://doi.org/10.1016/j.molp.2016.09.013.

Miettinen, Karel, Lemeng Dong, Nicolas Navrot, Thomas Schneider, Vincent Burlat, Jacob Pollier, Lotte Woittiez, et al. 2014. "The Seco-Iridoid Pathway from Catharanthus Roseus." *Nature Communications* 5 (3606). https://doi.org/10.1038/ncomms4606.

Murata, Jun, Jonathon Roepke, Heather Gordon, and Vincenzo De Luca. 2008. "The Leaf Epidermome of Catharanthus Roseus Reveals Its Biochemical Specialization." *Plant Cell* 20 (3): 524–42. https://doi.org/10.1105/tpc.107.056630.

Pan, Qifang, Natali Rianika Mustafa, Kexuan Tang, Young Hae Choi, and Robert Verpoorte. 2016. "Monoterpenoid Indole Alkaloids Biosynthesis and Its Regulation in Catharanthus Roseus: A Literature Review from Genes to Metabolites." *Phytochemistry Reviews* 15 (2): 221–50. https://doi.org/10.1007/s11101-015-9406-4.

Patron, Nicola J. 2020. "Beyond Natural: Synthetic Expansions of Botanical Form and Function." *New Phytologist* 227 (2): 295–310. https://doi.org/10.1111/nph.16562.

Patron, Nicola J., Diego Orzaez, Sylvestre Marillonnet, Heribert Warzecha, Colette Matthewman, Mark Youles, Oleg Raitskin, et al. 2015. "Standards for Plant Synthetic Biology: A Common Syntax for Exchange of DNA Parts." *New Phytologist* 208: 13–19.

Payne, Richard M.E., Deyang Xu, Emilien Foureau, Marta Ines Soares Teto Carqueijeiro, Audrey Oudin, Thomas Dugé De Bernonville, Vlastimil Novak, et al. 2017. "An NPF Transporter Exports a Central Monoterpene Indole Alkaloid Intermediate from the Vacuole." *Nature Plants* 3 (January): 1–9. https://doi.org/10.1038/nplants.2016.208.

Qu, Yang, Michael E.A.M. Easson, Razvan Simionescu, Josef Hajicek, Antje M.K. Thamm, Vonny Salim, and Vincenzo De Luca. 2018. “Solution of the Multistep Pathway for Assembly of Corynanthean, Strychnos, Iboga, and Aspidosperma Monoterpenoid Indole Alkaloids from 19E-Geissoschizine.” *Proceedings of the National Academy of Sciences of the United States of America* 115 (12): 3180–85. https://doi.org/10.1073/pnas.1719979115.

Reed, James, Michael J. Stephenson, Karel Miettinen, Bastiaan Brouwer, Aymeric Leveau, Paul Brett, Rebecca J.M. Goss, Alain Goossens, Maria A. O’Connell, and Anne Osbourn. 2017. “A Translational Synthetic Biology Platform for Rapid Access to Gram-Scale Quantities of Novel Drug-like Molecules.” *Metabolic Engineering* 42: 185–93. https://doi.org/10.1016/j.ymben.2017.06.012.

Rin, Soriya, Sayaka Imano, Maurizio Camagna, Takamasa Suzuki, Aiko Tanaka, Ikuo Sato, Sotaro Chiba, Kazuhito Kawakita, and Daigo Takemoto. 2020. “Expression Profiles of Genes for Enzymes Involved in Capsidiol Production in Nicotiana Benthamiana.” *Journal of General Plant Pathology* 86 (5): 340–49. https://doi.org/10.1007/s10327-020-00931-5.

Rodríguez-López, Carlos E., Benke Hong, Christian Paetz, Yoko Nakamura, Konstantinos Koudounas, Valentina Passeri, Luciana Baldoni, Fiammetta Alagna, Ornella Calderini, and Sarah E. O’Connor. 2021. “Two Bi-Functional Cytochrome P450 CYP72 Enzymes from Olive (Olea Europaea) Catalyze the Oxidative C-C Bond Cleavage in the Biosynthesis of Secoxy-Iridoids – Flavor and Quality Determinants in Olive Oil.” *New Phytologist* 229 (4): 2288–2301. https://doi.org/10.1111/nph.16975.

Saiman, Mohd Zuwairi, Karel Miettinen, Natali Rianika Mustafa, Young Hae Choi, Robert Verpoorte, and Anna Elisabeth Schulte. 2018. “Metabolic Alteration of Catharanthus Roseus Cell Suspension Cultures Overexpressing Geraniol Synthase in the Plastids or Cytosol.” *Plant Cell, Tissue and Organ Culture* 134 (1): 41–53. https://doi.org/10.1007/s11240-018-1398-5.

Sainsbury, Frank, Eva C. Thuenemann, and George P. Lomonossoff. 2009. “PEAQ: Versatile Expression Vectors for Easy and Quick Transient Expression of Heterologous Proteins in Plants.” *Plant Biotechnology Journal* 7 (7): 682–93. https://doi.org/10.1111/j.1467-7652.2009.00434.x.

Schmidt, Axel, Betty Wächtler, Ulrike Temp, Trygve Krekling, Armand Séguin, and Jonathan Gershenzon. 2010. “A Bifunctional Geranyl and Geranylgeranyl Diphosphate Synthase Is Involved in Terpene Oleoresin Formation in Picea Abies.” *Plant Physiology* 152 (2): 639–55. https://doi.org/10.1104/pp.109.144691.

Schultz, Bailey J., Seung Yeon Kim, Warren Lau, and Elizabeth S. Sattely. 2019. “Total Biosynthesis for Milligram-Scale Production of Etoposide Intermediates in a Plant Chassis.” *Journal of the American Chemical Society* 141 (49): 19231–35. https://doi.org/10.1021/jacs.9b10717.

Simkin, Andrew J., Karel Miettinen, Patricia Claudel, Vincent Burlat, Grégory Guirimand, Vincent Courdavault, Nicolas Papon, et al. 2013. “Characterization of the Plastidial Geraniol Synthase from Madagascar Periwinkle Which Initiates the Monoterpenoid Branch of the Alkaloid Pathway in Internal Phloem Associated Parenchyma.” *Phytochemistry* 85: 36–43. https://doi.org/10.1016/j.phytochem.2012.09.014.

Song, Chun Peng, Yan Guo, Quansheng Qiu, Georgina Lambert, David W. Galbraith, André Jagendorf, and Jian Kang Zhu. 2004. “A Probable Na+(K+)/H+ Exchanger on the Chloroplast Envelope Functions in PH Homeostasis and Chloroplast Development in Arabidopsis Thaliana.” *Proceedings of the National Academy of Sciences of the United States of America* 101 (27): 10211–16. https://doi.org/10.1073/pnas.0403709101.

Stavrinides, Anna, Evangelos C. Tatsis, Lorenzo Caputi, Emilien Foureau, Clare E.M. Stevenson, David M. Lawson, Vincent Courdavault, and Sarah E. O’Connor. 2016. “Structural Investigation of Heteroyohimbine Alkaloid Synthesis Reveals Active Site Elements That Control Stereoselectivity.” *Nature Communications* 7 (May): 1–14. https://doi.org/10.1038/ncomms12116.

Stephenson, Michael J., James Reed, Nicola J. Patron, George P. Lomonossoff, and Anne Osbourn. 2020. “Engineering Tobacco for Plant Natural Product Production.” In *Comprehensive Natural Products III: Chemistry and Biology*, edited by Hung-Wen (Ben) Liu and Tadhg P. Begley, 3rd ed., 6:244–62. Elsevier Ltd. https://doi.org/10.1016/b978-0-12-409547-2.14724-9.

Ting, Hieng Ming, Bo Wang, Anna Margareta Rydén, Lotte Woittiez, Teun Van Herpen, Francel W.A. Verstappen, Carolien Ruyter-Spira, Jules Beekwilder, Harro J. Bouwmeester, and Alexander Van der Krol. 2013. “The Metabolite Chemotype of Nicotiana Benthamiana Transiently Expressing Artemisinin Biosynthetic Pathway Genes Is a Function of CYP71AV1 Type and Relative Gene Dosage.” *New Phytologist* 199 (2): 352–66. https://doi.org/10.1111/nph.12274.

Trenti, Francesco, Kotaro Yamamoto, Benke Hong, Christian Paetz, Yoko Nakamura, and Sarah E.

O'Connor. 2021. "Early and Late Steps of Quinine Biosynthesis." *Organic Letters* 23 (5): 1793–97. https://doi.org/10.1021/acs.orglett.1c00206.

Wang, Bo, Arman Beyraghdar Kashkooli, Adrienne Sallets, Hieng Ming Ting, Norbert C.A. de Ruijter, Linda Olofsson, Peter Brodelius, et al. 2016. "Transient Production of Artemisinin in Nicotiana Benthamiana Is Boosted by a Specific Lipid Transfer Protein from A. Annua." *Metabolic Engineering* 38: 159–69. https://doi.org/10.1016/j.ymben.2016.07.004.

Wang, Quan, Shihai Xing, Qifang Pan, Fang Yuan, Jingya Zhao, Yuesheng Tian, Yu Chen, Guofeng Wang, and Kexuan Tang. 2012. "Development of Efficient Catharanthus Roseus Regeneration and Transformation System Using Agrobacterium Tumefaciens and Hypocotyls as Explants." *BMC Biotechnology* 12 (34): 1–12. https://doi.org/10.1186/1472-6750-12-34.

Yamamoto, Kotaro, Dagny Grzech, Konstantinos Koudounas, Emily Amor Stander, Lorenzo Caputi, Tetsuro Mimura, Vincent Courdavault, and Sarah E O'Connor. 2021. " Improved Virus-Induced Gene Silencing Allows Discovery of a Serpentine Synthase Gene in Catharanthus Roseus ." *Plant Physiology*, 1–12. https://doi.org/10.1093/plphys/kiab285.

Yamamoto, Kotaro, Katsutoshi Takahashi, Lorenzo Caputi, Hajime Mizuno, Carlos E. Rodriguez-Lopez, Tetsushi Iwasaki, Kimitsune Ishizaki, et al. 2019. "The Complexity of Intercellular Localisation of Alkaloids Revealed by Single-Cell Metabolomics." *New Phytologist* 224 (2): 848–59. https://doi.org/10.1111/nph.16138.

Yamamoto, Kotaro, Katsutoshi Takahashi, Hajime Mizuno, Aya Anegawa, Kimitsune Ishizaki, Hidehiro Fukaki, Miwa Ohnishi, Mami Yamazaki, Tsutomu Masujima, and Tetsuro Mimura. 2016. "Cell-Specific Localization of Alkaloids in Catharanthus Roseus Stem Tissue Measured with Imaging MS and Single-Cell MS." *Proceedings of the National Academy of Sciences of the United States of America* 113 (14): 3891–96. https://doi.org/10.1073/pnas.1521959113.

Supplementary Figure S1. Early metabolites of the iridoid pathway are derivatised by endogenous enzymes from *N. benthamiana*.

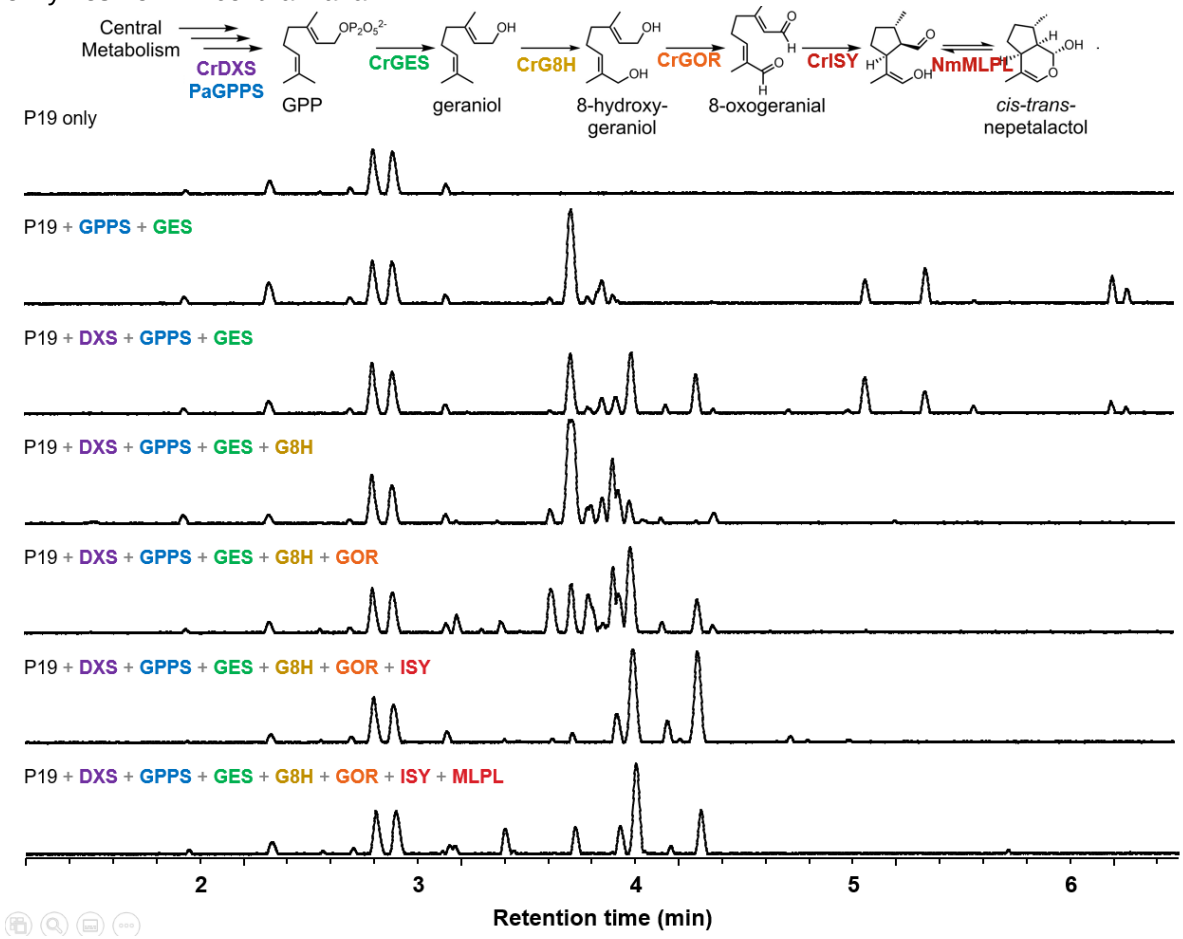

Supplementary Figure S2. Detection of 7-deoxyloganic acid by transient expression in *N. benthamiana*

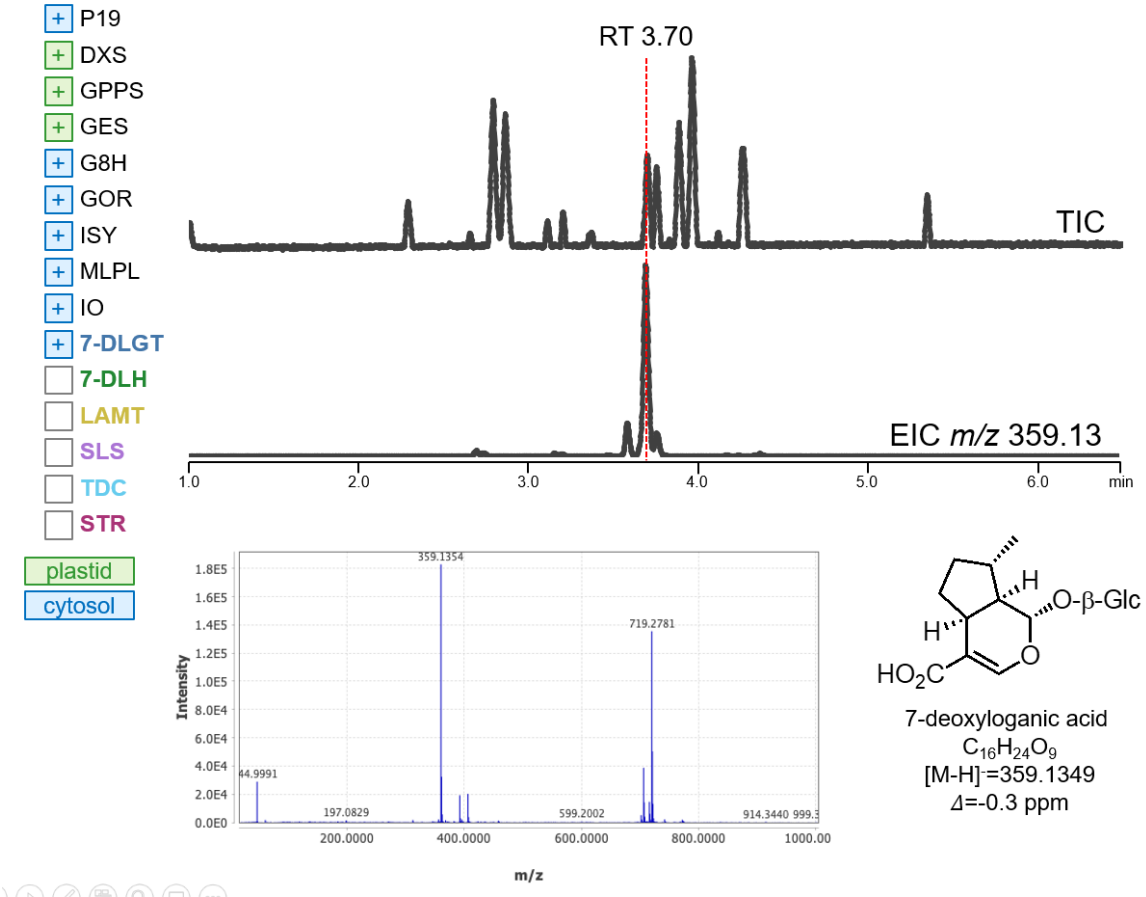

Supplementary Figure S3. Detection of loganic acid by transient expression in *N. benthamiana*

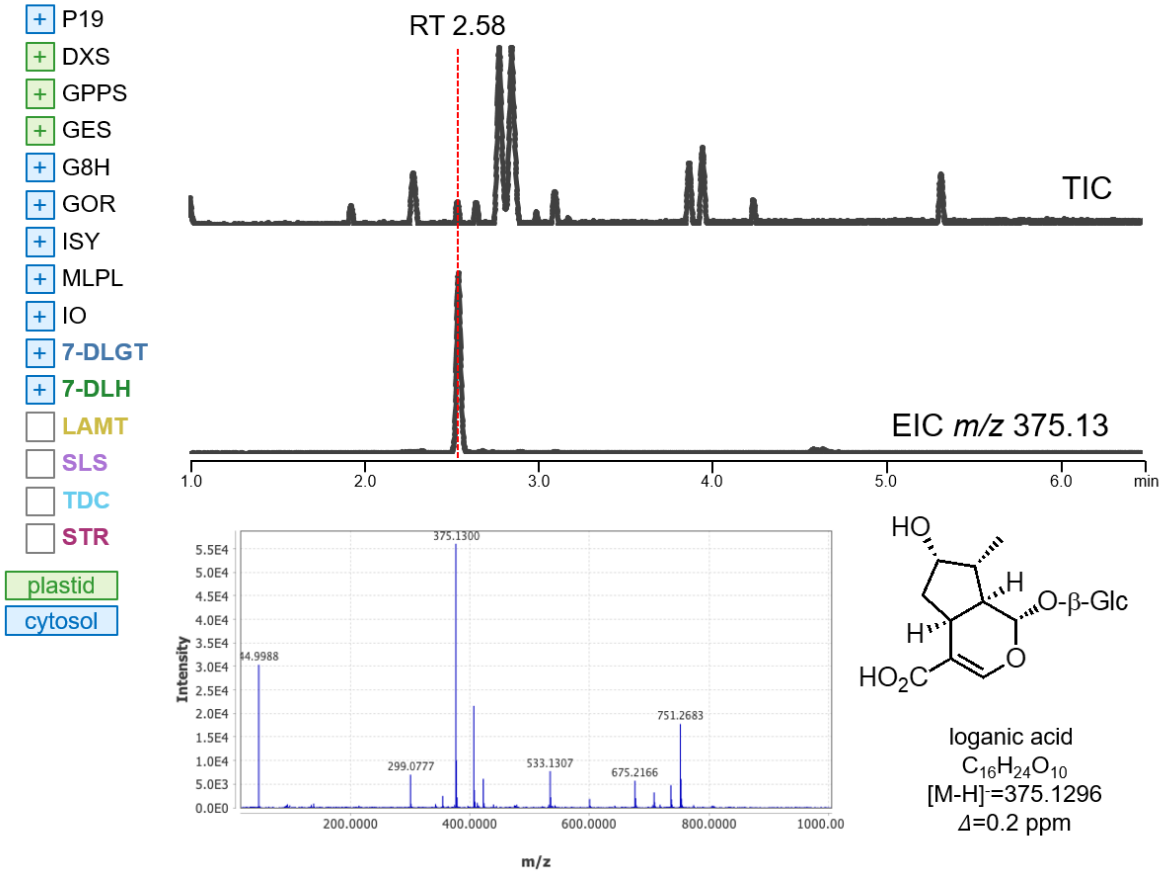

Supplementary Figure S4. Detection of loganin by transient expression in *N. benthamiana*

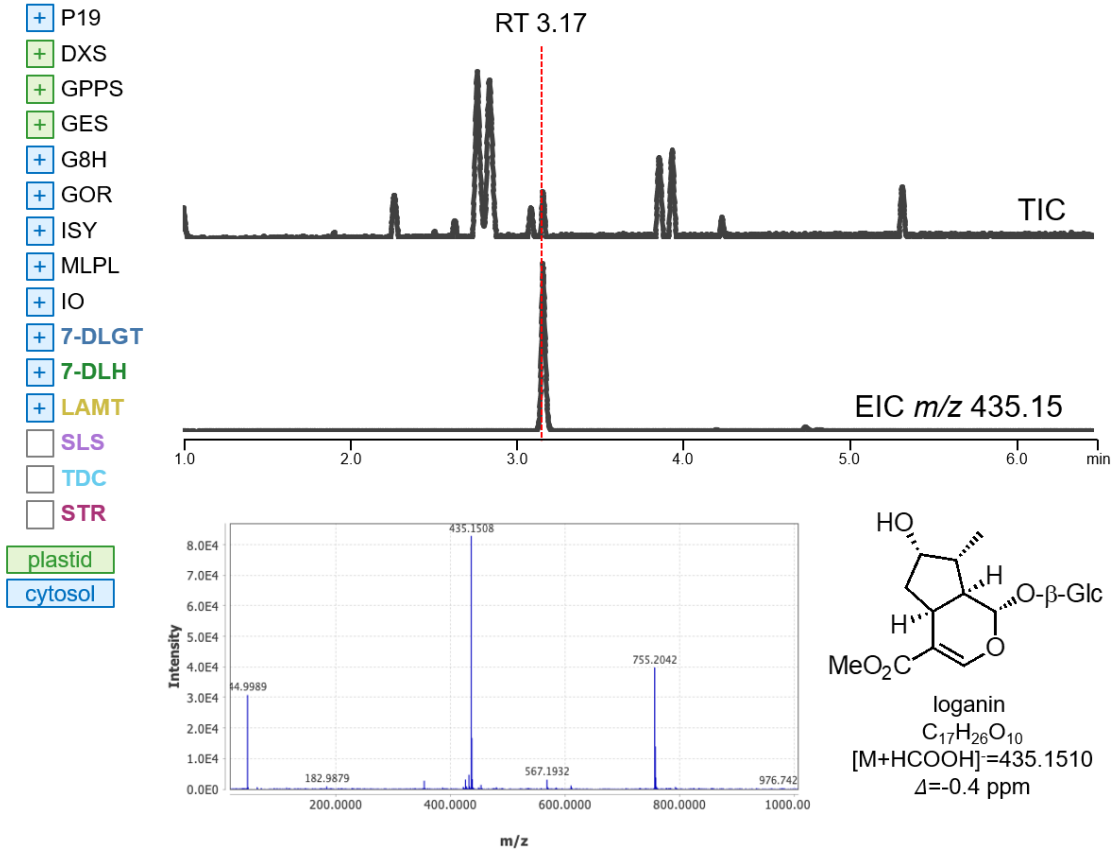

Supplementary Figure S5. Detection of strictosidine by transient expression in *N. benthamiana*

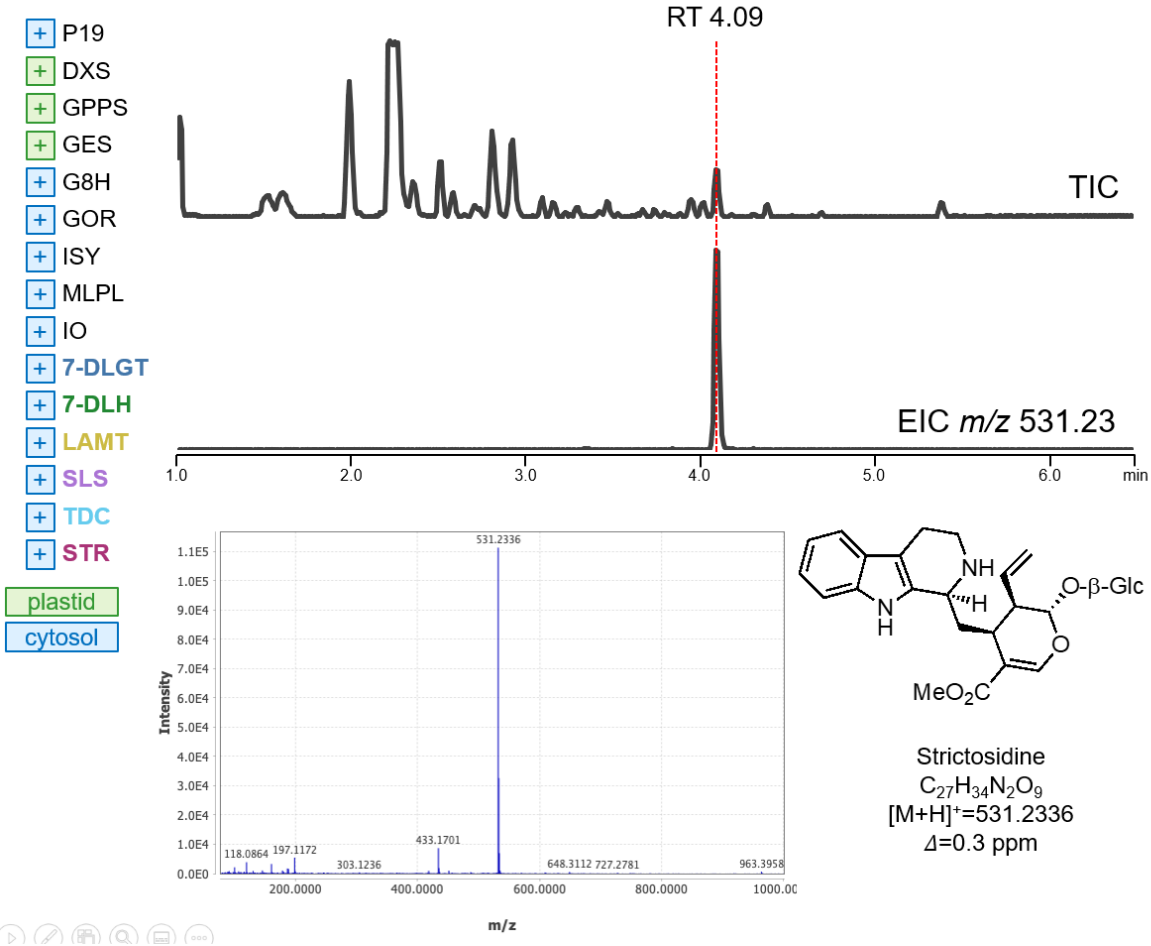

Supplementary Figure S6. Detection of malonyl-strictosidine by transient expression in *N. benthamiana*

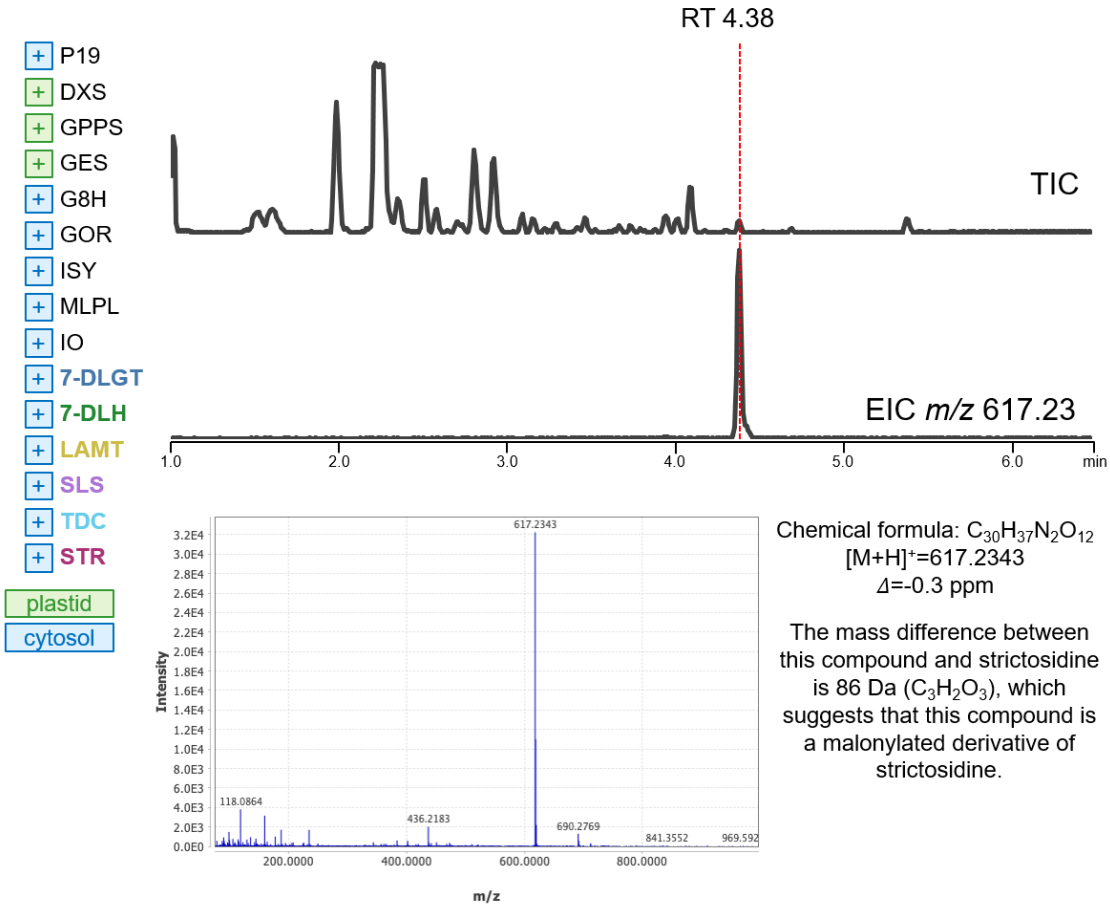

Chemical formula: $C_{30}H_{37}N_2O_{12}$
$[M+H]^+$=617.2343
Δ=-0.3 ppm

The mass difference between this compound and strictosidine is 86 Da ($C_3H_2O_3$), which suggests that this compound is a malonylated derivative of strictosidine.

Supplementary Figure S7. Amino acid sequence alignment of candidate GPPS enzymes

*PaGPPS1: GQ369788.1 – bifunctional GPPS and GGPPS, see Schmidt *et al.*, releases substantial portion of GPP
PgGPPS: AHE15048.1, used by Dudley *et al.* in plasmid 347_pJL1-(CAT7aa)-GPPS_Pgl
PaGPPS2: ACA21458.2, used by Dudley *et al.* in plasmid 287_pJL1-(CAT5aa)-GPPS2_Pab

* Used in this study as well as Miettinen *et al.* and Dong *et al.*

Schmidt *et al. Plant Physiology* 152:2 693-655 (2010)
Dudley *et al. Metab. Eng.* 61 251-260 (2020)
Miettinen *et al. Nat. Comm.* 5:3606 (2014)
Dong *et al. New Phytologist* 209:2 679-690 (2016)

Supplementary Table S1. Enzymes and L0 plasmid parts built in this study

Enzyme	Enzyme name	Organism	Abbreviation	Key reference(s)	GenBank Accession #	Level 0 plasmid name (AATG-GCTT)	Addgene #	Notes
DXS	1-deoxy-D-xylulose 5-phosphate synthase	*Catharanthus roseus* (Madagascar periwinkle)	CrDXS2	*this study*	DQ848672	pEPQD0CM0065	tbd	transit peptide removed, amplified from cDNA, contains R414K, T533A, A592T mutations relative to DQ848672.1
tHMGR	truncated 3-hydroxy-3-methylglutaryl-coenzyme A reductase	*Avena strigosa* (oat)	AstHMGR1	*2017 Reed, Osbourn, Metabolic Engineering* 42: 185–93	KY284573	pL0-AstHMGR *	tbd	truncated
GPPS	geranyl pyrophosphate synthase; geranyl diphosphate synthase	*Picea abies* (Norway spruce)	PaGPPS1	*2010 Schmidt, Gershenzon, Plant Physiology 152(2): 639–55*	GQ369788	pEPQD0CM0818	tbd	transit peptide removed
GES	geraniol synthase	*Catharanthus roseus* (Madagascar periwinkle)	CrGES	*2013 Simkin, Memelink, Clastre Phytochemistiry 85:36-43*	JN882024	pEPQD0CM0063	tbd	transit peptide removed
G8H (G10H)	geraniol 8-oxidase; geraniol-10-hydroxylase; CYP76B6	*Catharanthus roseus* (Madagascar periwinkle)	CrG8H	*2001 Collu FEBS Lett 508(2):215-220*	AJ251269	pEPQD0CM0058	tbd	
GOR (8-HGO, 10HGO)	8-hydroxygeraniol oxidoreductase; 10-hydroxygeraniol oxidoreductase; alcohol dehydrogenase 10	*Catharanthus roseus* (Madagascar periwinkle)	CrGOR	*2014 Miettinen, Werck-Reichhart Nat Comm 5:3606; 2015 Krithika, Thulasiram Sci Rep 5 8258*	KF302069	pEPQD0CM0059	tbd	
ISY (IRS, IS)	iridoid synthase	*Catharanthus roseus* (Madagascar periwinkle)	CrISY	*2012 Geu-Flores, O'Connor Nature 492(7427):138-142*	JX974564	pEPQD0CM0060	tbd	
MLPL	major latex protein–like	*Nepeta mussinii (aka Nepeta racemosa)*	NmMLPL	*2020 Lichman, O'Connor Sci Adv 6(20) eaba0721; 2019 Lichman, O'Connor Nat Chem Bio 15 71-79*	MT108267.1	pEPQD0CM0068	tbd	
IO	iridoid oxidase; CYP76A26	*Catharanthus roseus* (Madagascar periwinkle)	CrIO	*2014 Miettinen, Werck-Reichhart Nat Comm 5:3606; 2014 Salim, De Luca Phytochemistry 101:23-31*	KF302066	pEPQD0CM0061	tbd	amplified from cDNA, contains T359S relative to KF302066
7-DLGT	7-deoxyloganetic acid glucosyl transferase; UGT709C2	*Catharanthus roseus* (Madagascar periwinkle)	Cr7-DLGT	*2014 Miettinen, Werck-Reichhart Nat Comm 5:3606; 2013 Asada Plant Cell 25(10):4123-4134*	KF302068	pEPQD0CM0062	tbd	
7DLH	7-deoxyloganic acid hydroxylase; CYP72A224	*Catharanthus roseus* (Madagascar periwinkle)	Cr7DLH	*2014 Miettinen, Werck-Reichhart Nat Comm 5:3606; 2013 Salim, De Luca Plant J 76(5):754:765*	KF302067	pEPQD0CM0762	tbd	
LAMT	loganic acid O-methyltransferase	*Catharanthus roseus* (Madagascar periwinkle)	CrLAMT	*2008 Murata, De Luca Plant Cell 20(3):524-542*	EU057974	pEPQD0CM0763	tbd	
SLS	secologanin synthase; CYP72C	*Catharanthus roseus* (Madagascar periwinkle)	CrSLS1	*2000 Irmler, Schroder Plant J 24(6):797-804*	KF309242.1 or KF415117.1	pEPQD0CM0764	tbd	labeled SLS1 by 2015 Brown, O'Connor, PNAS 112(11) 3205-3210 and 2015 Qu, De Luca PNAS 112(19) 6224-6229; labeled by SLS2 de 2015 Bernonville, Courdavault, BMC Genomics 16(1) 619
TDC	tryptophan decarboxylase	*Catharanthus roseus* (Madagascar periwinkle)	CrTDC	*1989 De Luca, Brisson PNAS 86(8):2582-2586*	M25151	pEPQD0CM0765	tbd	
STR	strictosidine synthase	*Catharanthus roseus* (Madagascar periwinkle)	CrSTR	*1992 Pasquali, Memelink Plant Mol Biol 18(6):1121-1131*	X61932	pEPQD0CM0766	tbd	

* pL0-AstHMGR was a generous gift from Anne Osbourn

Supplementary Table S2. Level 1 plasmids for *A. tumefaciens* - mediated transient expression in *N. benthamiana*

	Promoter + 5' UTR + cTP(opt)		**CDS**	**3'UTR + Terminator**	**Level 1 Acceptor**
	GGAG-TACT	TACT-AATG	AATG-GCTT	GCTT-CGCT	CGCT-GGAG
pEPQD1CB0104 (P6_35SshortTMV-P19-35Sterm)	pICH51277		pICH44022	pUAP41414	pICH47781
pEPQD1CB0817 (P1_35SshortTMV-AstHMGR-35Sterm)	pICH51277		pL0-AstHMGR	pUAP41414	pICH47732
pEPQD1CB0107 (P1_ 35SshortTMV-cTP_CrDXS2-35Sterm)	pICH41388	pICH78133	pEPQD0CM0065	pUAP41414	pICH47732
pEPQD1CB0108 (P2_35SshortTMV-PaGPPS1-35Sterm)	pICH51277		pEPQD0CM0818	pUAP41414	pICH47742
pEPQD1CB0109 (P2_35SshortTMV-cTP_PaGPPS1-35Sterm)	pICH41388	pICH78133	pEPQD0CM0818	pUAP41414	pICH47742
pEPQD1CB0110 (P3_35SshortTMV-CrGES-35Sterm)	pICH51277		pEPQD0CM0063	pUAP41414	pICH47751
pEPQD1CB0112 (P3_35SshortTMV-cTP_CrGES-35Sterm)	pICH41388	pICH78133	pEPQD0CM0063	pUAP41414	pICH47751
pEPQD1CB0113 (P4_35SshortTMV-CrG8H-35Sterm)	pICH51277		pEPQD0CM0058	pUAP41414	pICH47761
pEPQD1CB0114 (P4_35SshortTMV-cTP_CrG8H-35Sterm)	pICH41388	pICH78133	pEPQD0CM0058	pUAP41414	pICH47761
pEPQD1CB0115 (P5_35SshortTMV-Cr8HGO/GOR-35Sterm)	pICH51277		pEPQD0CM0059	pUAP41414	pICH47772
pEPQD1CB0116 (P5_35SshortTMV-cTP_Cr8HGO/GOR-35Sterm)	pICH41388	pICH78133	pEPQD0CM0059	pUAP41414	pICH47772
pEPQD1CB0117 (P6_35SshortTMV-CrISY-35Sterm)	pICH51277		pEPQD0CM0060	pUAP41414	pICH47781
pEPQD1CB0118 (P6_35SshortTMV-cTP_CrISY-35Sterm)	pICH41388	pICH78133	pEPQD0CM0060	pUAP41414	pICH47781
pEPQD1CB0119 (P1_ 35SshortTMV-NmMLP-35Sterm)	pICH51277		pEPQD0CM0068	pUAP41414	pICH47732
pEPQD1CB0120 (P1_ 35SshortTMV-cTP_NmMLP-35Sterm)	pICH41388	pICH78133	pEPQD0CM0068	pUAP41414	pICH47732
pEPQD1CB0121 (P2_35SshortTMV-CrIO-35Sterm)	pICH51277		pEPQD0CM0061	pUAP41414	pICH47742
pEPQD1CB0122 (P2_35SshortTMV-cTP_CrIO-35Sterm)	pICH41388	pICH78133	pEPQD0CM0061	pUAP41414	pICH47742
pEPQD1CB0123 (P3_35SshortTMV-CrDLGT-35Sterm)	pICH51277		pEPQD0CM0062	pUAP41414	pICH47751
pEPQD1CB0124 (P3_35SshortTMV-cTP_CrDLGT-35Sterm)	pICH41388	pICH78133	pEPQD0CM0062	pUAP41414	pICH47751
pEPQD1CB0767 (P4_35SshortTMV-Cr7DLH-35Sterm)	pICH51277		pEPQD0CM0762	pUAP41414	pICH47761
pEPQD1CB0768 (P4_35SshortTMV-cTP_Cr7DLH-35Sterm)	pICH41388	pICH78133	pEPQD0CM0762	pUAP41414	pICH47761
pEPQD1CB0769 (P5_35SshortTMV- CrLAMT-35Sterm)	pICH51277		pEPQD0CM0763	pUAP41414	pICH47772
pEPQD1CB0770 (P5_35SshortTMV-cTP_ CrLAMT-35Sterm)	pICH41388	pICH78133	pEPQD0CM0763	pUAP41414	pICH47772
pEPQD1CB0771 (P6_35SshortTMV- CrSLS-35Sterm)	pICH51277		pEPQD0CM0764	pUAP41414	pICH47781
pEPQD1CB0772 (P6_35SshortTMV-cTP_ CrSLS-35Sterm)	pICH41388	pICH78133	pEPQD0CM0764	pUAP41414	pICH47781
pEPQD1CB0773 (P1_35SshortTMV- CrTDC-35Sterm)	pICH51277		pEPQD0CM0765	pUAP41414	pICH47732
pEPQD1CB0774 (P1_35SshortTMV-cTP_ CrTDC-35Sterm)	pICH41388	pICH78133	pEPQD0CM0765	pUAP41414	pICH47732
pEPQD1CB0775 (P2_35SshortTMV- CrSTR-35Sterm)	pICH51277		pEPQD0CM0766	pUAP41414	pICH47742
pEPQD1CB0776 (P2_35SshortTMV-cTP_ CrSTR-35Sterm)	pICH41388	pICH78133	pEPQD0CM0766	pUAP41414	pICH47742

Level 0 parts from MoClo kit
pICH51277 (CMV 35S short promoter + TMV omega 5'UTR) Addgene#50268
pICH41388 (CMV 35S short promoter) Addgene#50253
pICH78133 (TMV omega 5'UTR + synthetic chloroplast transit peptide RbcS) Addgene#50292
pUAP41414 (CMV 3'UTR + terminator) Addgene#50337
pICH44022 (L0, P19 CDS) Addgene#50330
pICH47732 (L1 P1 acceptor forward) Addgene#48000
pICH47742 (L1 P2 acceptor forward) Addgene#48001
pICH47751 (L1 P3 acceptor forward) Addgene#48002
pICH47761 (L1 P4 acceptor forward) Addgene#48003
pICH47772 (L1 P5 acceptor forward) Addgene#48004
pICH47781 (L1 P6 acceptor forward) Addgene#48005

Abbreviations
CMV = Cauliflower mosaic virus
TMV = Tobacco Mosaic Virus
P19 suppressor of gene silencing (Tomato Bushy Stunt Virus)
cTP = chloroplast transit peptide